Microsystem Technologies (2021) 27:833–842
https://doi.org/10.1007/s00542-020-05005-2

TECHNICAL PAPER

Realization of sucrose sensor using 1D photonic crystal structure vis-à-vis band gap analysis

Abinash Panda[1] · Puspa Devi Pukhrambam[1] · Gerd Keiser[2]

Received: 4 June 2020 / Accepted: 18 August 2020 / Published online: 26 August 2020

Abstract
A 1D photonic crystal based biosensor is explored for effective sensing of sucrose concentration in an aqueous solution. The proposed structure is realized with SOI based $LiNbO_3$–air–$LiNbO_3$ configuration, where thickness of $LiNbO_3$ and air layer are considered as 650 nm and 350 nm respectively. Reflected light energy from the structure is computed through analysis of a photonic band gap (PBG) by employing finite difference time domain technique. Simulations are carried out for investigation of shifts in reflected wavelength, PBG edges, PBG width, diffraction loss, reflected light energy, transmitted light energy, sensitivity and limit of detection (LOD) with reference to various sucrose concentrations. From the comparative analysis of vital sensing parameters with the existing researches, the proposed photonic sensor shows better sensitivity and low LOD which is suitable for bio sensing applications.

1 Introduction

Photonic crystals (PCs) are modern class of unique structures, which can amend the transmission of electromagnetic waves over a wide frequency range and therefore able to attract a great deal of research interest. Owing to their extraordinary optical properties, PC-based devices have received remarkable attention in sensing, networking and communication applications (Panda et al. 2016; 2019; Ramanujam et al. 2019). PCs integrated on SOI platform offers certain benefits like lower parasitic capacitance effect, low leakage current, high speed operation (Soref 1998; Colinge 1991; Peters 1993). SOI based photonic devices deliver unmatched optical properties due to high refractive index contrast between silicon substrate and oxide layer (Soref et al. 1991; Fischer et al. 1995). Thus, SOI structures with different types of materials, play key role in photonic integrated circuits for numerous photonics applications like interconnect, filter, sensor (Tidmarsh and Drake 1998; Yariv and Yeh 1984; Yablonovitch and Gmitter 1989; Zengerle and Leminger 1995; Tamir 1990). PCs are special structures based on periodic alternation in refractive index, in the order of wavelength of the propagating light signal. The periodic change in the dielectric function leads to considerable modification in both the transmission and reflectance spectrum. Moreover, the photonic crystal structures are blessed with a novel property, i.e. a photonic band gap (PBG), which prohibits the propagation of certain frequencies of the electromagnetic waves through the structure (Armenise et al. 2010; Nayak et al. 2016). This PBG phenomenon can be judiciously utilised for envisaging novel optical sensors for monitoring biomolecules, atmospheric gases, chemicals, temperature, and pressure (Penget et al. 2017; Panda and Pukhrambam 2020).

Among different compound materials used in the design of PCs, lithium niobate ($LiNbO_3$) has come up as a potential material for application in nonlinear and integrated optics. $LiNbO_3$ has been proven as a mature material for monitoring the flow of light signals in photonic devices (Arizmendi 2017; Liang et al. 2017). Owing to its high purity, $LiNbO_3$ has become the first choice of researchers for the design of novel optoelectronic devices. In addition to this, $LiNbO_3$ shows photorefractive, ferroelectric, electro-optic and acousto-optic properties, which enable it to find successful applications in optical and microwave frequency ranges (Geiss 2011). Also, $LiNbO_3$ shows some exceptional photonic band gap characteristics, which make

✉ Abinash Panda
abinashpanda087@gmail.com

[1] Department of Electronics and Communication Engineering, National Institute of Technology, Silchar, Assam 788010, India

[2] Department of Electrical Engineering, Boston University, Boston, MA 02215, USA

it a suitable candidate for the design of highly efficient optoelectronic devices such as optical switches, optical modulators, photochemical sensors, and photonic waveguides (Bernal et al. 2009; Prakash et al. 2019). $LiNbO_3$ based photonic crystal structures can find extensive applications in the field of biosensing (Christoph et al. 2015; Manpreet and Chetan 2014; Buswell et al. 2008; Hugo et al. 1991; Ayyanar et al. 2018). Among different biomolecules, sucrose is one of the key elements which is basically an aqueous solution of sugar and appears as a suitable component for creation of various chemical products like glycerol, ethanol, and citric acid (Caballero 2003). Moreover, concentration of sucrose in an aqueous solution finds extensive applications in pharmaceutical measures such as preservation of protein and food. Hence, it is indispensable to accurately sense the sucrose concentration. Numerous researches have already been performed towards exploring sensing of different biomolecules by using photonic waveguides (Katz and Willner 2004; Chen et al. 2016), but there is little research on sensing sucrose concentrations, which makes the present investigation noteworthy. In Panda et al. (2016, 2018), the authors demonstrated a 1D photonic waveguide and lucidly analysed the effect of different kinds of losses that persist during transmission of light signals through the waveguide. Further, in references Amiri et al. (2019), Robinson and Dhanlaksmi (2016), Palai et al. (2018), Tang and Wang (2008) and Wang and Tang (2012), the authors have lucidly represented sensing of glucose, urea, sodium chloride, DNA, protein by using photonic structures for realising efficient photonic integrated circuits. Also, several photonics structures are proposed Xiaoxia et al. (2020), Frischeisen et al. (2008), Chow et al. (2004), Ge et al. (2013) and Dorfner et al. (2009) to sense various analytes with analysis of important sensing characteristics like sensitivity and limit of detection (LOD).

To the best of the authors' knowledge, very few researches have been carried out to date regarding FDTD approach for photonic band gap exploration, particularly for the 1D photonic crystal. In order to provide some clarification of the aforementioned issue, we have simulated a 1D photonic crystal through FDTD methodology to reveal the change in the band gap characteristics with respect to different concentrations of sucrose solution. Moreover, we have chosen the FDTD technique over other existing methods such as Plane Wave Expansion (PWE) and Transfer Matrix Method (TMM), owing to its simple analysis and accurate outcomes pertaining to the band gap investigation. Aside from this, the primary reason for selecting the 1D structure is its compactness, simplicity and cost effectiveness from the design point of view, which can be fabricated using available technologies. To uncover more on the claim of sensing through band gap analysis, we have proposed $LiNbO_3$ material in the design of various layers of the 1D PhC structure, which add novelty to this work as this is not tested in published works. Furthermore, detailed analysis of reflected light energy, transmitted light energy, diffraction loss, and shift in reflected wavelength, PBG edges and PBG width escalates the novelty of the present research. Finally, a comparative analysis in terms of sensitivity and LOD is specified to measure the sensing performance, where the superiority of the present research is clearly illustrated.

2 Proposed structure and method

Over the last two decades, researchers have experimented with different materials and studied their properties to design photonic crystal structures and suggested that the best suited materials can be hybrid compound materials owing to their notable properties. In this research, we have considered a $LiNbO_3$ compound material for designing the proposed structure, which shows simultaneously photorefractive, ferroelectric, electro optic and acoustic optic properties. 1D PCs already have been commercialised and can be certainly fabricated with the help of widely accepted methodologies. These techniques include e-beam lithography, FIB (focused ion beam) method, sol–gel techniques, physical vapour deposition (PVD), chemical vapour deposition (CVD), molecular beam epitaxy, and spin coating methods (Chen et al. 2004; Schürmann et al. 2006; Langer et al. 1999; Huaizhong et al. 2016). The aforesaid techniques have been widely accepted by the semiconductor industries for manufacturing high quality, high performance 1D structures and also the same have been nicely executed in researches discussed in the introduction section. Out of the aforementioned techniques, choosing most apposite method is really vital pertaining to the fabrication feasibility. As of now, spin coating technique has been extensively employed in fabrication of 1D layered structures. The foremost beauty of this method is that it can be applied to a wide variety of materials as well as nanoparticles and polymer solutions. In spin coating method, initially some precursor solution is put on a plane substrate and afterwards spin method is conducted for evaporation of solvents. An annealing process is followed to congeal the thin film. The thickness of the developed thin film can be well organised by precisely governing the rotation speed. Now, coming to the fabrication steps of the proposed structure, spin coating technique can be applied to form a $LiNbO_3$ layer on the top of the SOI structure. Afterwards, photolithography process can be used through the application of photoresist to dissolve the required portion of the layer, which forms the second layer (air). Focusing on the feasibility aspect of fabrication, spin

coating method is proven to be technically simple with greater controllability and cost effective for realization of 1D photonic structures as compared to the fabrication methods for higher dimensional photonic structures (El et al. 2011; Ravi Kanth Kumar et al. 2002; Desmond et al. 2012).

The proposed SOI based 1D photonic crystal structure is shown in the Fig. 1, which consists of three layers, out of which the outer layers are designed with a $LiNbO_3$ compound material and the inner layer is taken as air. The thicknesses of the outer layer and inner layer are taken as $d_1 = 650$ nm and $d_2 = 350$ nm, respectively, whereas their permittivity is considered as $\varepsilon_1 = 5.303$ and $\varepsilon_2 = 1$ respectively. The photonic structure is considered to be created by e-beam lithography on a silicon substrate of 1 mm thickness. Additionally, infiltration technique is used to put aqueous solution of different sucrose concentrations in the middle layer. Based on the variation in refractive index, different sucrose concentrations can be sensed with enhanced sensitivity by observing the reflected wavelength shift according to the experimental setup shown in the Fig. 2. Light having wavelength of 390 nm is emitted from a laser source and incident on the proposed structure. At his wavelength, the proposed structure shows higher refractive index contrast between the adjacent layers, which yields more band gap. Light from the laser source can be focused and collected from the waveguide through a microscope objective lens for maximising the coupling efficiency. The light signals which fall within the band gap get reflected and others get transmitted through the structure. The directions of incident, reflected and transmitted light are shown with arrows in Fig. 1. Further, the aqueous solution is infiltrated in the second layer (i.e. air) and the reflected light energy is measured with a power meter. The principal reason for choosing the above thicknesses of different layers of the photonic structure is that maximum band gap is attained only at this thickness values, whereas for other values of thickness, band gap gradually decreases. Aside this, optimising the proposed structure with this thicknesses, diffraction loss is mitigated, which smoothen the passage of light in the waveguide. Also, at the aforementioned structure parameters, the suggested structure shows linear variation of sensing parameters and hence behaves as a suitable sensor for sensing different sucrose concentrations in an aqueous solution.

3 Computational methodology

A 1D photonic sensor has been envisaged in this article to sense sucrose concentration in an aqueous solution through a band gap analysis, where the band gap is computed through dispersion relation by manipulating an FDTD method. Although various methods are available to address the band gap characteristics of photonic structures, the FDTD technique is a simple and efficient analysis method for assessing the band gap properties in photonic structures (Sukhoivanov and Guryev 2009). The FDTD computational technique lies on discretization of Maxwell's equations. Beside this, the FDTD method is quiet efficient to permit complete exploration of electromagnetic waves over an arbitrary time by discretizing Maxwell's equations, such that one can collect any required data from the wave. In addition to this, the FDTD method shows great potential to solve the electromagnetics simulations even for large problem dimensions. FDTD employs a time domain method, so a broad frequency range can be covered during simulations, which leads to easy treatment of nonlinear material properties.

The propagation of EM waves through the proposed 1D photonic crystal structure are governed by Maxwell equations, which can be expressed as:

$$\nabla \times \vec{E} = -\mu \frac{\partial \vec{H}}{\partial t} \tag{1}$$

$$\nabla \times \vec{H} = \varepsilon \frac{\partial \vec{E}}{\partial t} + \vec{J} \tag{2}$$

The above equations are employed as the backbone for calculation of different electric field and magnetic field components that persist in the proposed structure. By using Eqs. (1) and (2), the band structure for magnetic field components can be realised by solving Helmholtz's equation, which can be expressed as,

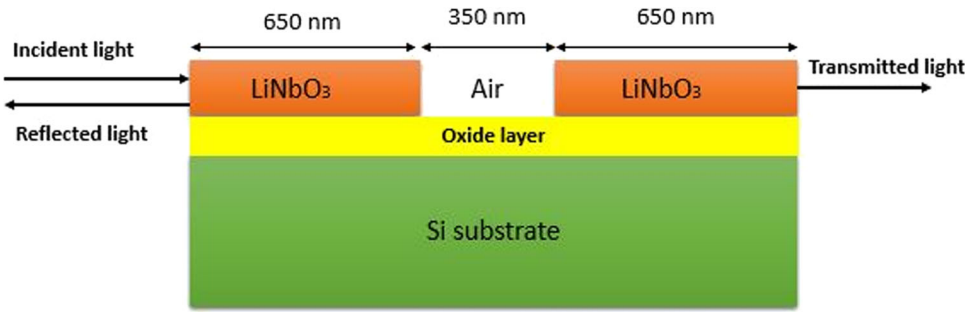

Fig. 1 Crossectional view of the proposed SOI based 1D PhC structure

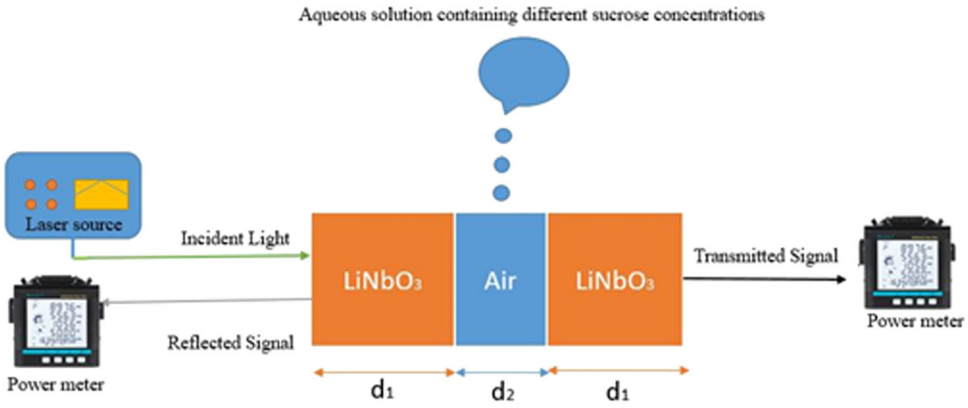

Fig. 2 Proposed experimental setup of sucrose sensor using 1D photonic structure

$$\frac{\partial}{\partial x}\frac{1}{\varepsilon(x)}\frac{\partial}{\partial x}H(x)+\frac{w^2}{c^2}H(x)=0 \tag{3}$$

where, H represents magnetic field component, c is the light speed, w denotes the Eigen frequency, ε(x) is the periodic dielectric function. Certain boundary conditions are applied for calculation of magnetic field component $H(x)$ with respect to different wave vectors. These boundary conditions are periodic in nature and referred as Bloch boundary conditions, which can expresses as below (Chhoker and Bajaj 2015),

$$H(x+a,y+b,z+c)=H(x,y,z).e^{-i.k_x.a-j.k_y.b-k.k_z.c} \tag{4}$$

where, a, b and c are dimension of unit cell along the x, y and z axis respectively, k_x, k_y and k_z, and represent the wave vectors along the corresponding axis. As per the present research, we have considered 1D PhC structure, which has periodicity variation along x axis only, so Eq. (4) reduces to

$$H(x+a)=H(x).e^{-i.k_x.a} \tag{5}$$

Thus, by considering Bloch periodic boundary conditions, it will be feasible to analyse Eigen states with respect to wave vector, which leads to computation of band structure (Sukhoivanov and Guryev 2009).

The rejected frequency range, i.e. band gap is further utilised to compute energy associated with the reflected light. In the above mentioned band gap analysis, the dielectric permittivity (ε) of $LiNbO_3$ is calculated using the expression (Zelmon et al. 1997),

$$\varepsilon=1+\frac{2.6734\times\lambda^2}{\lambda^2-0.01764}+\frac{1.2290\times\lambda^2}{\lambda^2-0.05914}+\frac{12.614\times\lambda^2}{\lambda^2-474.60} \tag{6}$$

The reflected light energy (E_r) can be obtained by utilising the following expression (Nayak et al. 2016),

$$E_r=\frac{h\times c}{\lambda_{up}-\lambda_{lo}} \tag{7}$$

where, λ_{up} and λ_{lo} denote the upper wavelength bound and lower wavelength bound of the attained band gap respectively, h represents the plank's constant and c is the speed of light.

After computation of reflected intensity from the obtained band gap, the diffraction loss (Panda et al. 2016) can be expressed as

$$D_{loss}=1-sin^2\left(\frac{\pi dn}{\lambda}\right) \tag{8}$$

where d represents the thickness of the proposed waveguide, n denotes refractive index and λ is the reflected wavelength, which lies within the band gap.

The transmitted energy through the proposed structure can be obtained by using the following expression (Swain et al. 2020),

$$E_T=(E_I-E_r)e^{-(\alpha t+\beta d)} \tag{9}$$

where E_T represents the transmitted energy, E_I denotes the incident light energy corresponding to the wavelength 390 nm, E_r is the reflected light energy. Further, the factor $e^{-(\alpha t+\beta d)}$ is the total absorption factor, which includes absorption due to both material ($e^{-\alpha t}$) and analytes ($e^{-\beta d}$), where α is the attenuation coefficient of $LiNbO_3$, t is the thickness of the $LiNbO_3$ grating. The factor $e^{-\beta d}$ can be expressed in simplified form as $e^{-\varepsilon cd}$, where ε is the extinction coefficient of sucrose, c and d denote the sucrose concentration and thickness of the middle layer of the proposed structure respectively. As the value of $e^{-\beta d}$ is very small as compared to $e^{-\alpha t}$, so absorption factor due to the analytes is neglected in the calculations.

Furthermore, we computed the sensitivity (S) parameter to appraise the performance of the proposed sensor, which is given as (Shaban et al. 2017):

$$S=\frac{\Delta\lambda_S}{\Delta n} \tag{10}$$

Here, $\Delta\lambda_S$ represents the shift in resonance wavelength and Δn is the change in refractive index associated with different sucrose concentrations.

To judge the sensor performance and to compare it to the performance of other sensor techniques, it is useful to derive the limit of detection (LOD). This parameter is noteworthy because it is defined as the lowest quantity or concentration of a compound that can be reliably detected with a given analytical method. For the numerical computation of LOD, we utilised the losses incurred in the proposed structure like diffraction loss. Thus here the LOD indicates the quantity of analytes which can be distinguished with above 99% reliability, and can be represented as (Romain et al. 2015):

$$LOD = \frac{3 \in}{S} \tag{11}$$

where $\in$ represents the standard deviation of error of diffraction loss and S denotes the sensitivity of the sensor. The LOD result and the comparison with other sensing methods are given in Table 2 and are discussed in Sect. 4.

4 Results and discussions

To realise the sucrose sensor, initially a simulation is carried out by employing the FDTD computational technique towards investigating dispersion relation of the proposed waveguide structure. The dispersion relation indicates the variation of frequency with respect to wave vector, which can be altered by controlling different parameters such as refractive index of the material, number of grating layers, and width and thickness of the photonic waveguide. From a simulation point of view, the thickness of the outer layers ($LiNbO_3$) is taken to be 650 nm and thickness of the inner layer (air) is chosen to be 350 nm, whereas the width is taken as 100 nm. The refractive index for different concentrations of sucrose in the aqueous solution is acquired from Yunus (1988) and is listed in Table 1.

Referring to the different data listed in Table 1, simulations are carried out by deploying FDTD technique for analysis of dispersion relation between frequency and wave vector with reference to all the listed sucrose concentrations, which range from 10 g/100 ml to 70 g/100 ml. Simulation outcomes only for the low and high sucrose concentrations of 10 g/100 ml and 70 g/100 ml are depicted in this manuscript as the Figs. 3 and 4 respectively.

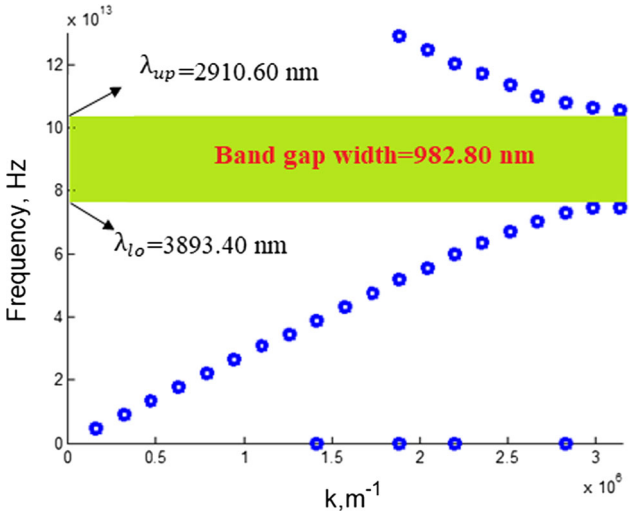

Fig. 3 Dispersion relation of frequency with wave vector for 10 g/100 ml sucrose concentration

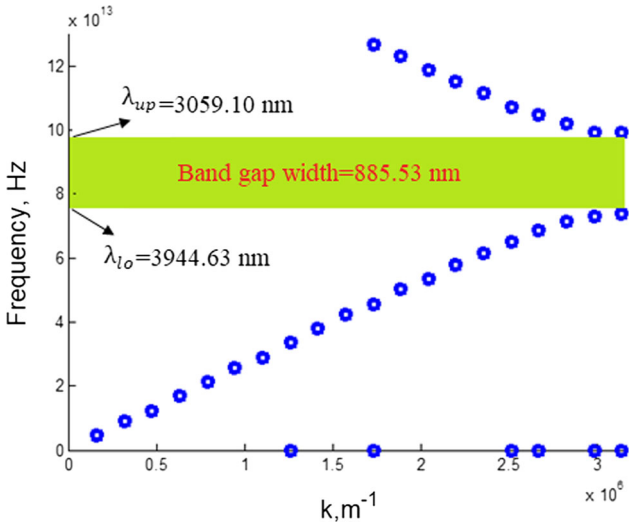

Fig. 4 Dispersion relation of frequency with wave vector for 70 g/100 ml sucrose concentration

In Figs. 3 and 4, frequency in Hz is plotted in the y-axis whereas wave vector k in m^{-1} is shown in the x-axis. The frequency gap is highlighted with green colour in the figures, which signifies the prohibited frequency range/band gap in the proposed photonic structure. From the highlighted frequency gap, the corresponding wavelength of upper and lower edge of the PBG is computed, and also the band gap width is calculated, which are indicated in the aforementioned figures.

Table 1 Refractive index information for different sucrose concentration

Sucrose concentration in g/100 ml	10	20	30	40	50	60	70
Refractive index	1.345	1.364	1.385	1.396	1.410	1.433	1.442

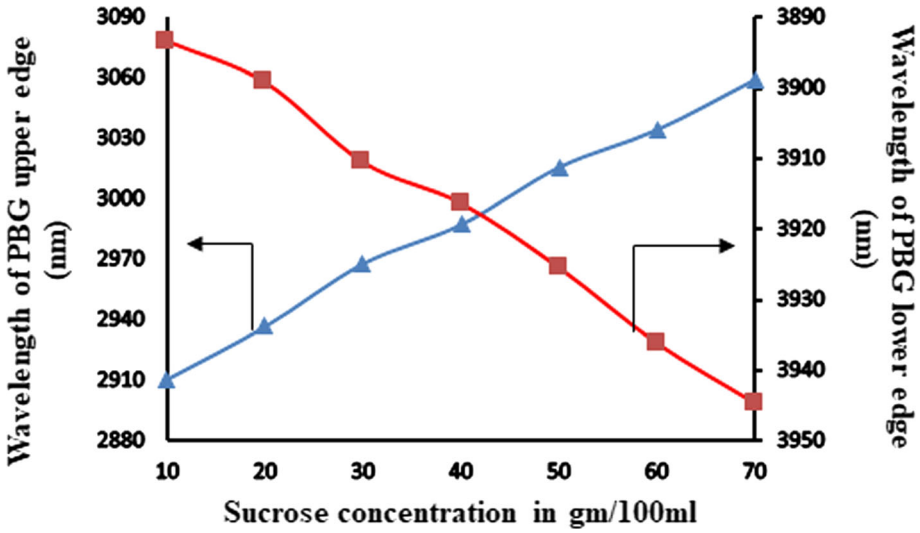

Fig. 5 Variation in wavelength of the PBG edge

Figure 5 represents the variation of wavelength associated with the upper edge and lower edge of the PBG, which are shown along the primary vertical axis and secondary vertical axis (reverse order), respectively. It is observed that wavelength of the upper edge varies from 2910.60 to 3059.10 nm whereas wavelength of the lower edge varies from 3893.40 to 3944.63 nm, with respect to different sucrose concentrations. This significant linear shift in the aforementioned PBG edge can be taken as a sensing parameter for the proposed sucrose sensor.

Further, we investigated the shift in the PBG width with reference to various sucrose concentrations, which is shown in Fig. 6. From this figure it can be seen that the width of the PBG decrease from 982.8 to 885.53 nm with respect to an increase in sucrose concentration from 10 g/100 ml to 70 g/100 ml. Interestingly, the variation in PBG width is nicely fitted with a linear trend line (R^2 = 0.9907), which ensures accurate sensing of sucrose concentrations.

In addition to this, the shifts in the central reflected wavelengths with respect to different sucrose concentrations are thoroughly studied and are presented in Fig. 7. It can be seen that the central reflected wavelength is shifted towards higher wavelength, i.e. from 3402 nm to 3501.86 nm, for increases in the sucrose concentrations. In addition to this, the above variations follow a highly linear trend with R^2 = 0.9979. This significant shift in the central reflected wavelength appears to be a key parameter to evaluate the performance of the sensor.

Afterwards, we analysed the sensor performance by investigating the sensitivity parameter using Eq. (10). Sensitivity is computed for different concentrations of sucrose with respect to pure water. Figure 8 shows the variation in sensitivity in nm/RIU along the vertical axis

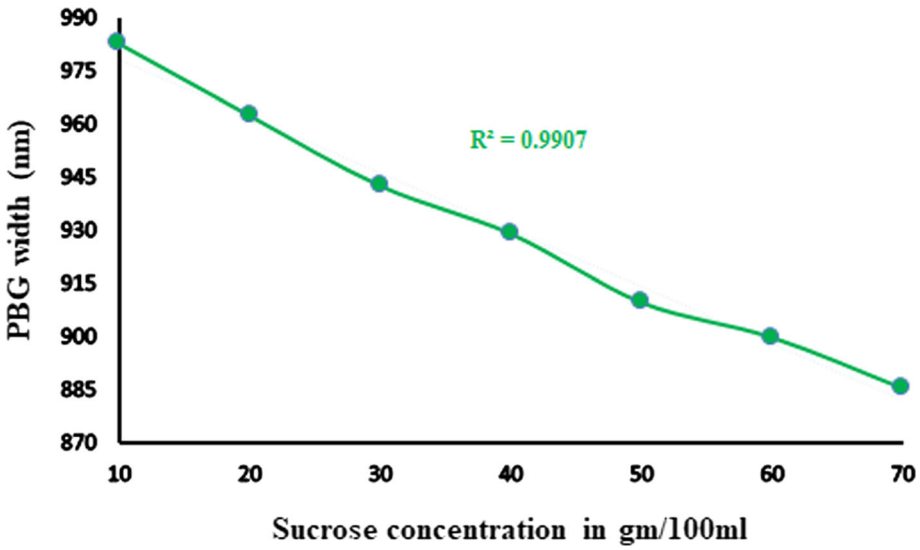

Fig. 6 Variation of PBG width with respect to sucrose concentrations

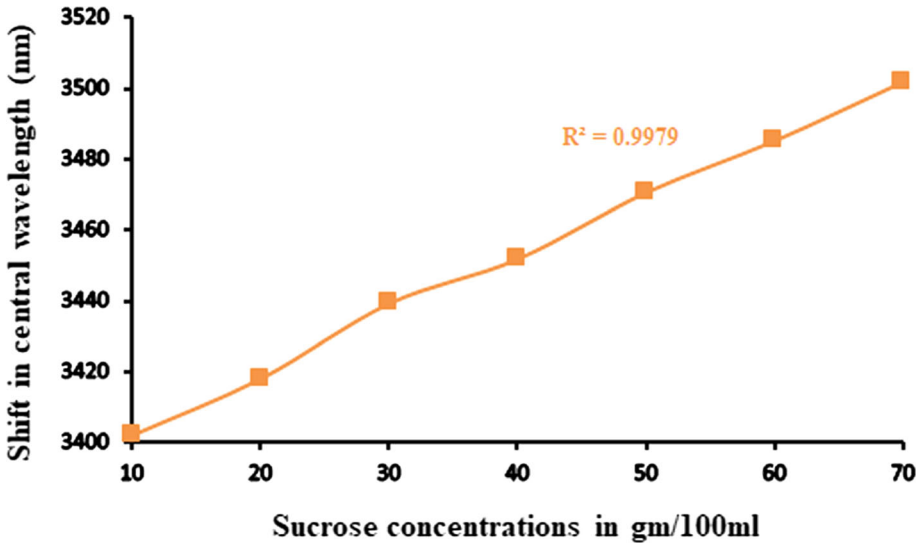

Fig. 7 Variation in the central reflected wavelength with respect to sucrose concentrations

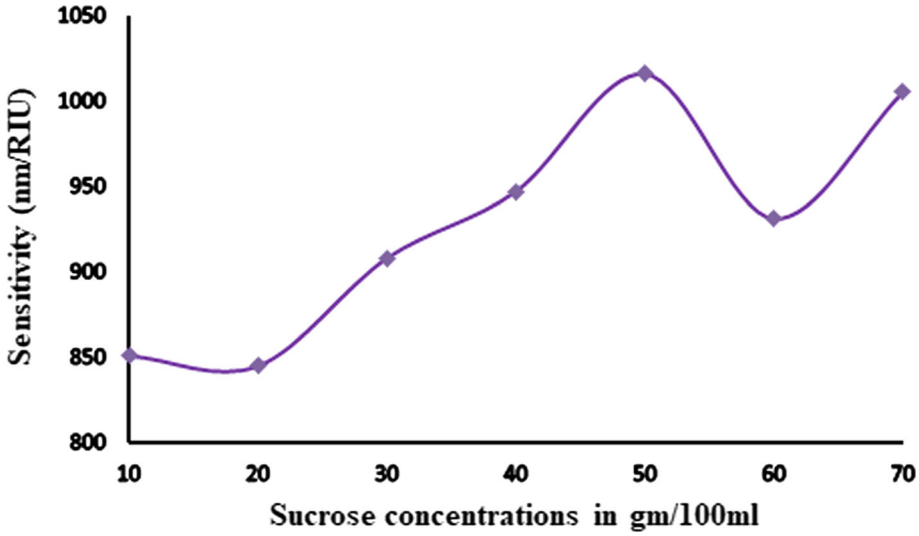

Fig. 8 Variation of sensitivity with respect to sucrose concentrations

whereas sucrose concentration in gm/100 ml is taken along the horizontal axis. A nonlinear variation in sensitivity is witnessed particularly for the case of 20 g/100 ml and 60 g/100 ml sucrose concentrations, which is due to relatively small change in wavelength shift ($\Delta\lambda_S$). Also, it has been found that a maximum sensitivity of 1016.35 nm/RIU is obtained for the proposed sensor, which proves its efficiency. Thereafter, we calculated the limit of detection of the proposed sensor with the help of Eq. (11), and we obtained a very low LOD of 2.28×10^{-4} RIU, which indicate that the proposed 1D PhC structure can minutely sense small changes in concentration of sucrose in aqueous solution. We have also compared different performance characteristics of the sensor with other researches available in the literature, which are stated in Table 2. From Table 2 it can be seen that the proposed sensor exhibits superb sensing characteristics in terms of sensitivity and LOD, with these parameters being comparable or slightly superior to other sensing techniques. However, other features of the proposed sensor (such as compactness, fabrication simplicity, and inexpensive manufacturing) make the present sensor configuration a very noteworthy contender.

Later, we calculated the variation in reflected light energy and transmitted light energy in the proposed structure through numerical formulations as explained in the Sect. 3, and the results are shown in Fig. 9. The primary vertical axis represents the shift in reflected light energy (E_r) with respect to different sucrose concentrations, where it is perceived that E_r decreases from 0.3649 to 0.3545 eV as the sucrose concentration varies from 10 g/100 ml to 70 g/100 ml. Similarly, the secondary vertical axis shows the variation in transmitted light energy (E_T), where a shift from 1.1443 to 1.1485 eV is marked in for different sucrose concentrations. Beside this, it also has

Table 2 Comparative analysis of sensor performance

Sl. no.	Structure	Analytes	Sensitivity	LOD	References
1	Polymer horizontal slot waveguide	Liquid (R.I. 1.3180–1.3184)	177 nm/RIU	1.69×10^{-4} RIU	Xiaoxia et al. (2020)
2	Kretschmann sensor	NaCl solution	–	6×10^{-4} RIU	Frischeisen et al. (2008)
3	2D PhC with defect	Glycerol	183 nm/RIU	–	Chow et al. (2004)
4	GMR on 1D grating	Biotin Estradiol	212 nm/RIU	–	Ge et al. (2013)
5	Photonic crystal nanostructure	Refractive index sensor	103 nm/RIU	2.4×10^{-3} RIU	Dorfner et al. (2009)
6	1D photonic crystal structure	Sucrose (10 g/100 ml to 70 g/100 ml)	1016.35 nm/RIU	2.28×10^{-4} RIU	Proposed work

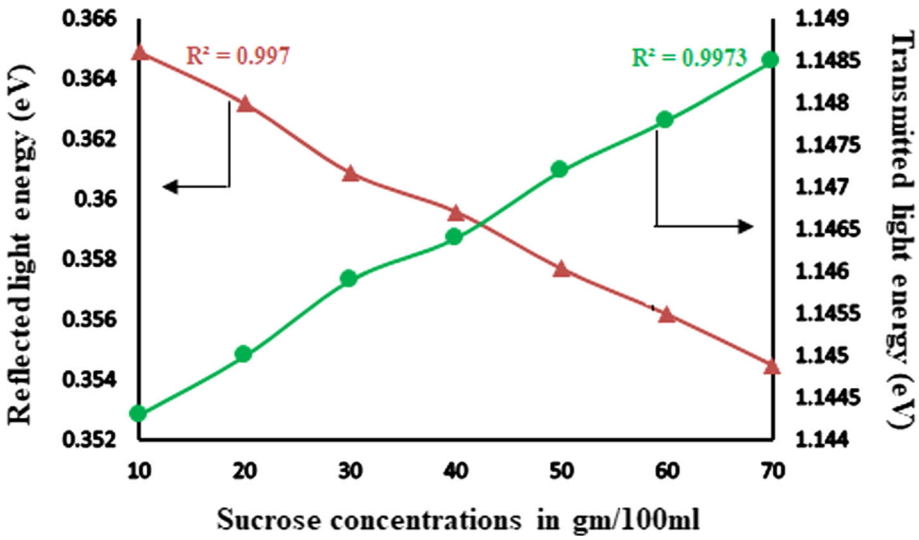

Fig. 9 Variation of reflected light energy and transmitted light energy with respect to sucrose concentrations

been asserted that variation of both E_r and E_T follow the linear trend line with correlation coefficients of $R^2 = 0.9970$ and $R^2 = 0.9973$ respectively, which deduce precise sensing of sucrose concentration by the proposed $LiNb0_3$ based 1D photonic crystal structure.

Finally, investigation on diffraction loss is carried out and it is found that there exist a definite amount of diffraction loss in the photonic crystal during propagation of a light signal, which is graphically shown in the Fig. 10. From this figure, we concluded that diffraction loss increases almost linearly from 0.152 to 0.69 Arbi.Unit with an increase in sucrose concentration.

5 Conclusions

The present research exhibits a simple yet efficient LiNb03 based 1D PhC structure for accurate sensing of different sucrose concentrations in an aqueous solution. The physics behind this research is bandgap analysis by employing an FDTD methodology with respect to various sucrose concentrations in the range 10 g/100 ml to 70 g/100 ml. Structure parameters like thickness of the PCs, refractive index of the material and height of the structure play vital roles to accomplish accurate sensing of sucrose concentrations. Sensing characteristics are realised through shift in reflected wavelength, PBG edges and PBG width with reference to variation in sucrose concentration. Furthermore, diffraction loss, reflected light energy and transmitted light energy in the proposed structure are examined, and a notable change is observed in the aforesaid parameters for different sucrose concentrations. Again, it has been divulged that variations of the aforementioned parameters nicely follow a linear trend line, which claims the proposed structure as a suitable candidate for accurate sensing of sucrose concentration in the aqueous solution. Finally, we compared sensitivity and LOD of the present research with reported researches in the literature and

Fig. 10 Variation of diffraction loss with respect to sucrose concentrations

concluded that the proposed sensor outperforms other methods in terms of above mentioned sensing parameters.

References

Amiri IS, Yupapin P, Palai G (2019) Estimation of concentration of DNA and protein through PARD and modified analysis: a realization of an accurate biomedical device using photonic structure. Optik 182:507–511

Arizmendi L (2017) Photonic applications of lithium niobate crystals. Phys Stat Sol 201:253–283

Armenise MN, Campanella CE, Ciminelli C, Olio FD, Passaro VMN (2010) Phononic and photonic band gap structures: modelling and applications. Phys Procedia 3:357–364

Ayyanar N et al (2018) Enhanced sensitivity of hemoglobin sensor using dual-core photonic crystal fiber. Opt Quantum Electron 50:453

Bernal MP, Roussey M, Baida F, Benchabane S, Khelif A, Laude V (2009) Photonic and phononic band Gap properties of lithium niobate, ferroelectric crystals for photonic applications. Springer series in materials science. Springer, Berlin

Buswell SC, Wright VA, Buriak JM, Van V, Evoy S (2008) Specific detection of proteins using photonic crystal waveguides. Opt Express 16:15949–15957

Caballero B (2003) Encyclopedia of food sciences and nutrition, 2nd edn. ISBN: 978-0-12-227055-0

Chen HL, Lee HF, Chao WC, Hsieh CI, Ko FH (2004) Fabrication of autocloned photonic crystals by using high-density-plasmachemical vapor deposition. Vac Sci Technol B 22:3359

Chen W et al (2016) Molecular imprinted photonic crystal for sensing of biomolecules. De Gruyter 4:1–12

Chhoker P, Bajaj S (2015) Analysis of photonic band structure in 1-D photonic crystal using PWE and FDTD Method. IJISET Int J Innov Sci Eng Technol 2:883–887

Chow E, Grot A, Mirkarimi LW, Sigalas M, Girolami G (2004) Ultracompact biochemical sensor built with two-dimension-alphotonic crystal microcavity. Opt Lett 29:1093–1095

Christoph F et al (2015) Photonic crystal based sensing scheme for acetylchloline and acetylcholinesterase inhibitors. J Mater Chem B 3:2089–2095

Colinge JP (1991) Silicon-on-insulator technology: materials to VLSI. Kluwer Academic, Boston

Desmond M, Sandoghchi SR, Adikan RM (2012) Fabrication of photonic crystal fibers. In: 3rd international conference on photonics (ICP 2012), Penang, Malaysia, pp 227–230. https://doi.org/10.1109/ICP.2012.6379830

Dorfner D et al (2009) Photonic crystal nanostructures for optical biosensing applications. Biosens Bioelectron 24:3688–3692

El HH, Laurent B, Geraud B, Igor R, Mohamed B, Bruno C (2011) From molecular precursors in solution to microstructured optical fiber: a sol–gel polymeric route. Opt Mater Express 1:234–242

Fischer U, Zinke T, Petermann K (1995) Integrated optical waveguide switches in SOI. In: 1995 IEEE international SOI conference proceedings, Tucson, AZ, USA, pp 141–142. https://doi.org/10.1109/SOI.1995.526500

Frischeisen J, Mayr C, Reinke NA, Nowy S, Brütting W (2008) Surface plasmon resonance sensor utilizing an integrated organic light emitting diode. Opt Express 16:18426–18436

Ge C et al (2013) External cavity laser biosensor. Lab Chip 13:1247–1256

Geiss R et al (2011) Transmission properties of a free-standing lithium niobate photonic crystal waveguide. In: CLEO: 2011—Laser science to photonic applications, Baltimore, MD, USA, pp 1–2. https://doi.org/10.1364/CLEO_SI.2011.CFI4

Huaizhong S, Zhanhua WW, Yuxin YB (2016) One-dimensional photonic crystals: fabrication, responsiveness and emerging applications in 3D construction. RSC Adv 6:4505–4520

Hugo S et al (1991) Light scattering in lntralipid-10% in the wavelength range of 400–1100 nm. Appl Opt 30:4507–4514

Katz E, Willner I (2004) Integrated nanoparticle-biomolecule hybrid systems: synthesis, properties, and applications. Angew Chem Int Ed 43:6042–6108

Langer R, Barski A, Simon J, Pelekanos NT, Konovalov O, Andre R, Dang LS (1999) High-reflectivity GaN/GaAlN Bragg mirrors at blue/green wavelengths grown by molecular beam epitaxy. Appl Phys Lett 74:3610–3612

Liang H, Luo R, He Y, Jiang H, Lin Q (2017) High-quality lithium niobate photonic crystal nanocavities. Optica 4:1251–1258

Manpreet C, Chetan S (2014) Design of a photonic crystal biosensor using DNA filled microcavity and ring cavity coupled with waveguide. In: 2014 international conference on signal propagation and computer technology (ICSPCT 2014), Ajmer, India, pp 342–345. https://doi.org/10.1109/ICSPCT.2014.6885026

Nayak C, Palai G, Sarkar P (2016) Investigation of mole fraction in nitride semiconductor using photonic bandgap analysis. Optik 127:697–699

Palai G, Kisan S, Das A (2018) A proposal for bio-medical device to measure GUS in human blood using metamaterial. Optik 164:138–142

Panda A, Pukhrambam PD (2020) Photonic crystal biosensor for refractive index based cancerous cell detection. Opt Fiber Technol 54:102123

Panda A, Mishra CS, Palai G (2016a) PWE approach to optical thyristor for investigation of doping concentration. Optik 127:4831–4833

Panda A, Sarkar P, Palai G (2016b) Studies on temperature variation in semiconductor waveguide through ARDP loss for nanophotonic applications. Optik 127:5439–5442

Panda A, Sarkar P, Palai G (2018) Research on SAD-PRD losses in semiconductor waveguide for application in photonic integrated circuits. Optik 154:748–754

Panda A, Pukhrambam PD, Keiser G (2019) Realization of sucrose sensor using photonic waveguide: an application to biophotonics. In: 2019 International workshop on fiber optics in access networks (FOAN), Sarajevo, Bosnia and Herzegovina, pp 23–25. https://doi.org/10.1109/FOAN.2019.8933813

Penget J et al (2017) Thin films based one-dimensional photonic crystal for humidity detection. Sens Actuator A Phys 263:209–215

Peters L (1993) SOI takes over where silicon leaves off. Semicond Int 16:48–51

Prakash S, Sharma G, Yadav GC et al (2019) Photonic band gap alteration in $LiNbO_3$–SiO_2 Based 1D periodic multilayered structure via plate wave. Silicon 11:1783–1789

Ramanujam NR et al (2019) Enhanced sensitivity of cancer cell using one dimensional nano composite material coated photonic crystal. Microsyst Technol 25:189–196

Ravi Kanth Kumar VV, George AK, Reeves WH, Knight JC, Russell PSJ (2002) Extruded soft glass photonic crystal fiber for ultrabroad supercontinuum generation. Opt Express 10:1520–1525

Robinson S, Dhanlaksmi N (2016) Photonic crystal based biosensor for the detection of glucose concentration in urine. Photonic Sens. https://doi.org/10.1007/s13320-016-0347-3

Romain G et al (2015) Sensitivity and limit of detection of biosensors based on ring resonators. Sens Biosens Res 6:99–102

Schürmann U, Takele H, Zaporojtchenko V, Faupel F (2006) Optical and electrical properties of polymer metal nanocomposites prepared by magnetron co-sputtering. Thin Solid Films 515:801–804

Shaban M et al (2017) Tunability and sensing properties of plasmonic/1D photonic crystal. Sci Rep 7:41983

Soref R (1998) Applications of silicon-based optoelectronics. MRS Bull 23:20–24

Soref RA, Schmidtchen J, Petermann K (1991) Large single-mode rib waveguides in GeSi and Si-on-SiO_2. IEEEJ Quantum Electron 27:1971–1974

Sukhoivanov IA, Guryev IV (2009) Physics and practical modeling: photonic crystals. Springer, Berlin

Swain KP, Nayyar A, Palai G, Tripathy SK (2020) Disseminating of bio-info with respect to different photonic crystal structure through AWS. Optik 202:163590

Tamir T (ed) (1990) Guided wave optoelectronics, 2nd edn. Springer, Berlin

Tang JL, Wang JN (2008) Chemical sensing sensitivity of long-period grating sensor enhanced by colloidal gold nanoparticles. Sensors 8:171–184

Tidmarsh J, Drake J (1998) Silicon-on-insulator waveguide bragg gratings. In: Integrated photonic research (IPR'98), vol 4 of OSA Technical Digest, Victoria, BC, Canada, pp 290–292

Wang JN, Tang JL (2012) Photonic crystal fiber Mach–Zehnder interferometer for Refractive Index sensing. Sensors 12:2983–2995

Xiaoxia MA, Kaixin C, Jieyun W, Lingfang W (2020) Low-cost and highly sensitive liquid Refractive Index sensor based on polymer horizontal slot waveguide. Photonic Sens 10:7–15

Yablonovitch E, Gmitter TJ (1989) Photonic band structure: the face centered-cubic case. Phys Rev Lett 63:1950–1953

Yariv A, Yeh P (1984) Optical waves in crystals. Wiley, New York

Yunus W (1988) Refractive index of solutions at high concentrations. Appl Opt 27:3341–3343

Zelmon DE, Small DL, Jundt D (1997) Infrared corrected Sellmeier coefficients for congruently grown lithium niobate and 5 mol% magnesium oxide-doped lithium niobate. J Opt Soc Am B 14:3319–3322

Zengerle R, Leminger O (1995) Phase shift bragg grating filters with improved transmission characteristics. J Light Wave Technol 13:2354–2358